

The Interaction of Alba, a Conserved Archaeal Chromatin Protein, with Sir2 and Its Regulation by Acetylation

Stephen D. Bell,^{1*} Catherine H. Botting,²
Benjamin N. Wardleworth,² Stephen P. Jackson,³
Malcolm F. White^{2*}

The conserved Sir2 family of proteins has protein deacetylase activity that is dependent on NAD (the oxidized form of nicotinamide adenine dinucleotide). Although histones are one likely target for the enzymatic activity of eukaryotic Sir2 proteins, little is known about the substrates and roles of prokaryotic Sir2 homologs. We reveal that an archaeal Sir2 homolog interacts specifically with the major archaeal chromatin protein, Alba, and that Alba exists in acetylated and nonacetylated forms. Furthermore, we show that Sir2 can deacetylate Alba and mediate transcriptional repression in a reconstituted *in vitro* transcription system. These data provide a paradigm for how Sir2 family proteins influence transcription and suggest that modulation of chromatin structure by acetylation arose before the divergence of the archaeal and eukaryotic lineages.

Although the archaeal basal transcription apparatus resembles the core of the eukaryotic RNA polymerase (RNAP) II apparatus, it is thought that regulation of gene expression in Archaea is effected by simple bacterial-like regulators [reviewed in (1)]. By contrast, in eukaryotes the modulation of chromatin structure by covalent modification of histones plays a pivotal role in transcriptional regulation (2). The Sir2 protein of budding yeast has an important role in chromatin dynamics, and this correlates with its ability to deacetylate histones *in vitro* (3, 4). It is intriguing that Sir2 family members not only are conserved among eukaryotes, but also are found in many bacterial and archaeal species (5). Although the three-dimensional (3D) crystal structure of an archaeal Sir2 homolog has been obtained (6), the physiological role and substrate(s) of the archaeal Sir2 proteins are not yet known.

We based our studies on *Sulfolobus solfataricus* P2, an archaeal species that encodes a single Sir2 homolog, ssSir2 (7). Recombinant ssSir2 [a wild-type and a mutant with a substitution of tyrosine for the histidine at

position 116 (H116Y)] were purified as hexa-His-tagged fusion proteins (8). The analogous mutation in yeast Sir2 is known to abolish its enzymatic activities (9, 10). The wild-type ssSir2 protein can deacetylate a heterologous substrate *in vitro* in an NAD-dependent manner, and additionally has a mono-ADP ribosyl transferase (MART) activity [Supplementary fig. 1 (8)]. When antisera raised against ssSir2 were used to probe Western blots of *Sulfolobus* whole-cell extracts, we detected a protein doublet migrating at ~27 kD (Fig. 1A). After gel-filtration chromatography, the lower form of the doublet elutes with a molecular mass of ~50 to 60 kD, whereas the upper form migrates as a monomer, similar to the recombinant protein

(Fig. 1A). As there is no evidence that Sir2 can dimerize in solution (Fig. 1A) (6), we suspected the change in apparent molecular mass was due to a stable interaction with another protein. ssSir2 has MART activity [Supplementary fig. 1 (8)], so we reasoned that the upper band in the doublet might correspond to a covalently modified form of ssSir2. To test this, we preincubated *Sulfolobus* extract with 200 μ M NAD before gel filtration. This resulted in an increase in the amount of the upper, monomeric form of the protein and a concomitant reduction in the intensity of the lower band, suggesting that an NAD-dependent modification of ssSir2 in the extract leads to disruption of the protein:protein interaction (Fig. 1B).

To identify the protein interacting with ssSir2, we coupled preimmune serum or antiserum elicited by immunization with ssSir2 to beads for use in immuno-affinity purification. High salt elution from the beads conjugated to ssSir2 antiserum yielded a single polypeptide of ~10 kD (Fig. 2A). This species was identified by mass fingerprinting as the major *Sulfolobus* chromatin protein, Sso10b (7, 11). This protein is highly conserved in archaeal genomes, and it is intriguing that clear sequence homologs are present in a range of eukaryotes. Eukaryotic homologs of Sso10b are apparent in most higher plants and protists such as *Leishmania* and trypanosome species. No recognizable homologs are present in fungi or *Caenorhabditis elegans*, although there are weaker homologs in vertebrates including *Homo sapiens* (Fig. 2B). This protein has been named according to the molecular weight and the species of origin: Sso10b from *Sulfolobus solfataricus*, Ssh10b from *Sulfolobus shibatae*, etc. (11). We propose a new name for the protein, Alba (acetylation lowers binding affinity; see below), to eliminate problems with nomenclature.

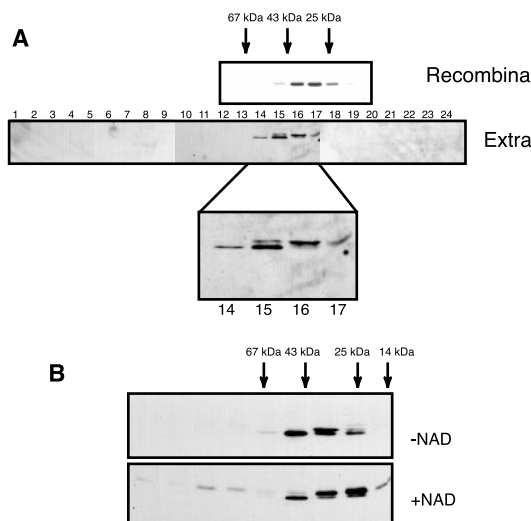


Fig. 1. *Sulfolobus* Sir2 exists in two forms in vivo. (A) Profile of recombinant ssSir2 (upper panel) and ssSir2 in cell extract (middle panel) on Superose 6 gel filtration chromatography. ssSir was detected by Western blotting of column fractions after SDS-polyacrylamide gel electrophoresis (SDS-PAGE). The position of peak elution of size standards is shown above the top panel. The lower panel shows a magnified view of fractions 14 to 17. (B) Effect of incubation of extract with 0 or 200 μ M of NAD for 30 min at 50°C before chromatography on Superose 6.

¹Medical Research Council (MRC) Cancer Cell Unit, The Hutchison/MRC Research Centre, Hills Road, Cambridge, CB2 2QH, UK. ²Centre for Biomolecular Sciences, St. Andrews University, North Haugh, St. Andrews, Fife, KY16 9ST, UK. ³Wellcome Trust and Cancer Research Campaign Institute of Cancer and Developmental Biology, Tennis Court Road, Cambridge, CB2 1QR, UK; and Department of Zoology, University of Cambridge, UK.

*To whom correspondence should be addressed. E-mail: sdb@mole.bio.cam.ac.uk and mfw2@st-andrews.ac.uk

REPORTS

To verify the interaction between Alba and ssSir2, we found that a recombinant GST-Alba fusion protein, but not GST alone, can interact with recombinant ssSir2 (Fig. 2C, left panel). The protein complex was resistant to the addition of ethidium bromide, indicating a direct interaction rather than one mediated by DNA. Furthermore, incubation of whole-cell extract with GST-Alba resulted in selective recovery of the lower species of the ssSir2 doublet (Fig. 2D), confirming the observation that only the unmodified version of ssSir2 is involved in the interaction. We next tested whether Alba might influence the enzymatic activities of ssSir2. However, incubation of recombinant Alba with

ssSir2 in either the presence or absence of DNA has no significant effect on either the deacetylase or MART activity of ssSir2 [Supplementary fig. 2 (8)].

Given the association of Alba with a conserved protein that alters covalent modification of eucaryal chromatin, we next investigated the possibility of covalent modification of Alba *in vivo*. To this end, we purified Alba from a *Sulfolobus* cell lysate. Purified native Alba was compared with recombinant Alba from *Escherichia coli* by matrix-assisted laser desorption time-of-flight (MALDI-TOF) mass spectrometry. Native Alba protein had a mass of

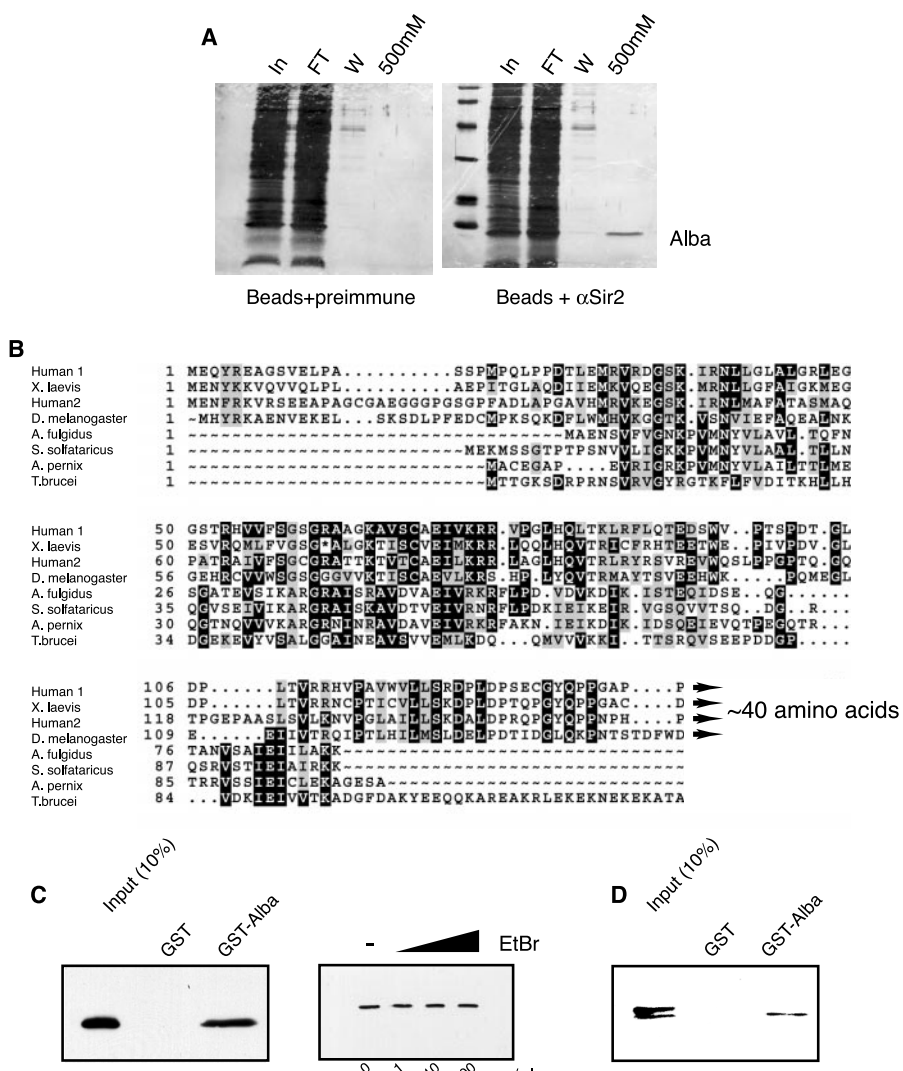


Fig. 2. Identification of Alba as a ssSir2 interaction partner. **(A)** Sir2 interacting protein was purified as described in (8). Samples of input (In), unbound material (FT), wash (W), and 500 mM NaCl eluate were electrophoresed, and the proteins were detected by silver-staining. **(B)** Sequence alignment of eucaryal and archaeal Alba homologs. **(C)** Interaction between GST-Alba and recombinant ssSir2 in vitro. Left panel: GST or GST-Alba (5 µg) immobilized on glutathione Sepharose beads were incubated with 2 µg of ssSir2. Right panel: GST-Alba (5 µg) was incubated with 2 µg of ssSir2 in the presence of the indicated amounts of ethidium bromide. After extensive washing, bound proteins were eluted by boiling in 1 × SDS-PAGE loading buffer. After electrophoresis, ssSir2 was detected by Western blotting. **(D)** Alba interacts with the faster migrating form of endogenous ssSir2. *S. solfataricus* extract (30 µg) was incubated with 5 µg of GST or GST-Alba. Samples were treated as above.

10,538 daltons, 84 mass units larger than the recombinant protein that has a mass of 10,454 daltons, as expected for the unmodified protein after removal of the NH₂-terminal methionine residue [Supplementary figs. 3 and 4 (8)]. This is consistent with the addition of two acetyl groups (42 mass units each) to the polypeptide chain. Native Alba was resistant to Edman degradation, suggesting that the NH₂-terminal serine residue is acetylated on the α -amino group. Tryptic digestion of native Alba resulted in the identification by mass spectrometry of a peptide with a mass of 1668.8 daltons, consistent with the NH₂-terminal peptide (SSGTPTPSNVVLIGKK) with two acetyl groups. As the NH₂-terminus is acetylated, the second acetylation site in this peptide is likely to be on the ϵ -amino group of Lys¹⁶, forcing trypsin to cleave after Lys¹⁷ even though the unfavored residue Pro¹⁸ is in the P'₁ position. Consequently, a significant proportion of the protein is not cut by trypsin in this region, resulting in the persistence of a larger peptide of mass 4136.8 daltons, corresponding to the doubly acetylated NH₂-terminal peptide cleaved at Lys⁴¹ (consistent with acetylation at the NH₂-terminus and either Lys¹⁷ or more probably Lys¹⁶). As expected, recombinant Alba shows no evidence of acetylation when digested by trypsin, allowing efficient cleavage after Lys¹⁶ to yield an unmodified NH₂-terminal peptide of mass 1456.6 daltons [Supplementary fig. 5 (8)].

Does acetylation affect the DNA binding characteristics of Alba? DNA binding affinities for both recombinant and acetylated Alba were measured by electrophoretic mobility-shift assay. The recombinant protein displayed highly cooperative binding with an apparent dissociation constant of ~ 30 nM (Fig. 3). By comparison, native doubly acetylated Alba bound in a similar cooperative manner but with a dissociation constant of 1.1 μM . This decrease in binding affinity by a factor of 30 was highly likely to be due to the acetylation of the native protein at Lys¹⁶ or Lys¹⁷. To test their importance for DNA binding, each of these residues was mutated to alanine and glutamate, and the resultant mutants tested for DNA binding affinity. Mutation of either lysine residue to alanine resulted in a significant decrease in DNA binding affinity (by a factor of 7 to 14), and replacement with glutamic acid resulted in an apparent dissociation constant reduced from that of the wild-type recombinant Alba by a factor of ~ 40 —similar to the acetylated native protein (Fig. 3).

The identification of Alba as an interaction partner for ssSir2 suggests that, as in eukaryotes, ssSir2 may have a role in chromatin modulation and may thereby impinge upon processes such as recombination, replication, and

transcription. We therefore tested the ability of recombinant Alba to influence a reconstituted *Sulfolobus* in vitro transcription system. Recombinant, nonacetylated Alba represses transcription of the SSV1 T6 promoter in vitro (Fig. 4A). In contrast, the addition of equivalent amounts of a second *Sulfolobus* chromatin protein, Sso7d, has no significant effect on transcription, indicating that the effect of Alba is specific. We next compared the ability of acetylated and nonacetylated Alba to mediate transcriptional repression. In striking contrast to unmodified Alba, acetylated Alba is unable to bring about significant transcriptional repression at the concentrations tested (Fig. 4B). Similarly, derivatives of recombinant Alba with point mutations at lysines 16 or 17 are unable to

repress transcription (Fig. 4C). Thus, there is a strong correlation between the measured binding affinity of Alba (Fig. 3) and its ability to mediate transcriptional repression.

In light of the above data, we reasoned that ssSir2 might deacetylate Alba and thereby modulate the ability of Alba to bind DNA and repress transcription. When we performed assays on naked DNA templates, we found that ssSir2 has no detectable effect on transcription (Fig. 4D). Next, we added acetylated Alba to DNA in the presence of ssSir2, ssSir2 H116Y, or buffer. As seen in Fig. 4E, no significant transcriptional repression occurs in the presence of ssSir2 H116Y or buffer control. By contrast, transcriptional repression is observed in the presence of ssSir2 on the acetylated Alba tem-

plate. Furthermore, transcriptional repression is dependent on the presence of both ssSir2 and its cofactor NAD (Fig. 4E, lower panel), suggesting that the deacetylation of Alba by ssSir2 is the crucial step mediating transcriptional repression.

In summary, we find that archaeal Sir2 forms a stable interaction with the major archaeal chromatin protein Alba. *In vivo*, a significant proportion of Alba is acetylated on lysine residues in the NH₂-terminal region of the protein and the effect of acetylation is to reduce the affinity of Alba for DNA. Our data support a role for ssSir2 in deacetylating Alba, resulting in an increase in Alba's DNA binding affinity, and thereby repressing transcription. The observation that ssSir2 both binds and deacetylates Alba suggests an attractive model for how an initial site of Alba-mediated transcriptional repression could spread to adjacent sites on the DNA template. Thus, by deacetylating non-DNA-bound Alba, ssSir2 would stimulate Alba-DNA interactions, leading to the recruitment of Alba and ssSir2 to DNA and the nucleation of further Alba deacetylation. This type of mechanism has the potential to establish regions of Alba-coated DNA, repressive to transcription and other processes. Such self-spreading phenomena have been observed with eukaryotic Sir2 and other chromatin modulatory proteins such as histone methyl transferases (4). Our results also strongly suggest that, in addition to having simple bacterial-like gene regulatory networks (1, 12), archaea also have the capacity to carry out regulation of DNA-based activities at the chromatin level. Ongoing studies of the archaeal chromatin modifying machinery may therefore shed further light on the evolution of the complex eukaryotic nuclear regulatory activities. In this regard, it is noteworthy that many eukaryotes, including humans, encode homologs of both Alba and Sir2, suggesting that this partnership

Protein	App. K _d (nM)
Native Alba	1100 ± 330
Rec. Alba	33 ± 10
K16A	220 ± 18
K16E	1300 ± 280
K17A	480 ± 90
K17E	1400 ± 300

Fig. 3. DNA binding affinity of Alba is modulated by acetylation. Recombinant Alba binds a 50-oligomer DNA duplex in a highly cooperative manner with an apparent dissociation constant of 33 nM (green), whereas the native acetylated protein (blue) also binds cooperatively, but more weakly (it has 1/30th the affinity). Mutants of recombinant Alba in which Lys¹⁶ or Lys¹⁷ have been changed to alanines (black) show intermediate binding affinities, whereas changes to glutamate (red) result in binding affinities similar to the acetylated protein. Binding isotherms were determined in triplicate, with standard errors indicated for each point.

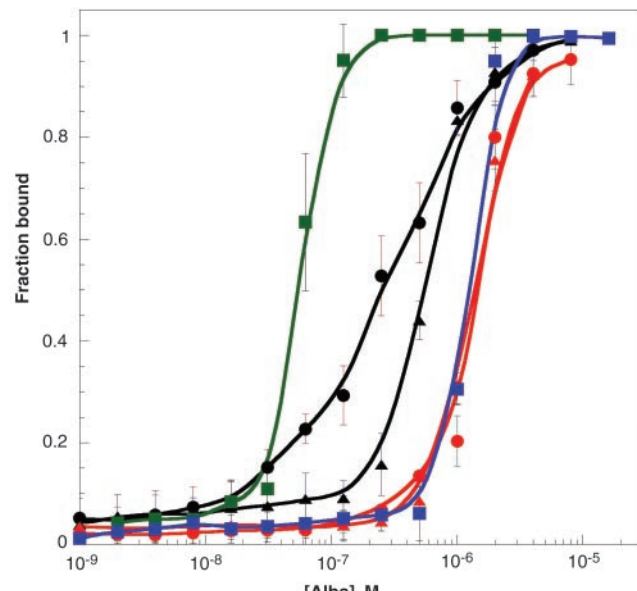
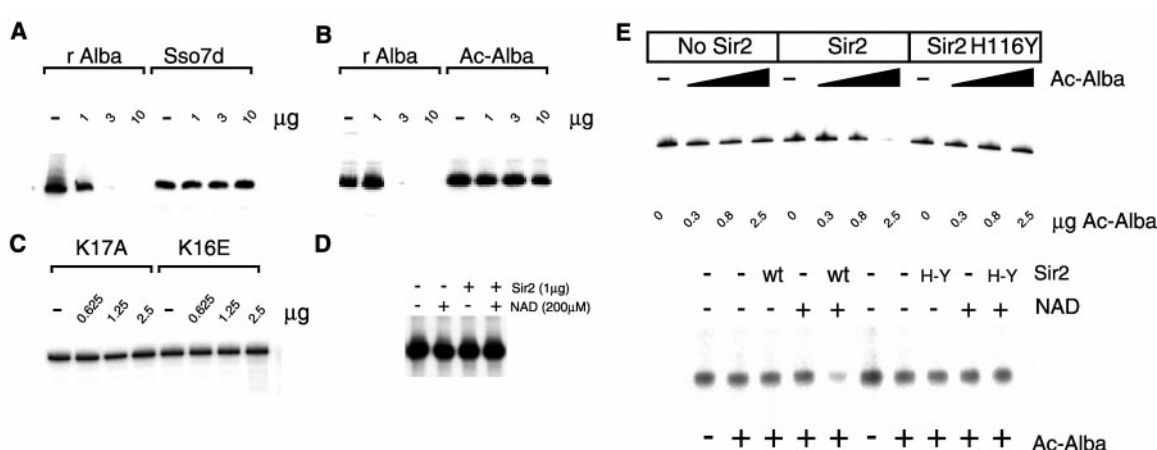


Fig. 4. ssSir2 mediates transcriptional silencing in vitro. (A) Transcription assays were performed on a template containing the T6 promoter of SSV1. Assay conditions were as described (13). (B) Transcription reactions were assembled with recombinant, nonacetylated (r), or acetylated (Ac) Alba. (C) Transcription reactions were assembled containing recombinant Alba with the indicated point mutations. (D) Transcription assays programmed with a plasmid containing the T6 promoter, supplemented with 1 μg of ssSir2 and/or 200 μM of NAD as indicated. (E) Upper panel: Transcription assays containing 200 μM of NAD were assembled on the T6 promoter template and incubated with Ac Alba in the presence of 1 μg of either ssSir2 or ssSir2 H116Y for 20 min at 65°C before the initiation of



transcription by addition of NTPs to 200 μM. Lower panel: Transcription assays were assembled on the T6 promoter in the presence or absence of 2.5 μg of acetylated Alba. Reactions were supplemented with NAD to 200 μM and/or ssSir2 [wild type (wt) or H116Y (H-Y)]. Reactions were preincubated as above.

REPORTS

may have been highly conserved throughout evolution.

References and Notes

1. S. D. Bell, S. P. Jackson, *Curr. Opin. Microbiol.* **4**, 208 (2001).
2. M. Grunstein, *Nature* **389**, 349 (1997).
3. L. Guarente, *Genes Dev.* **14**, 1021 (2000).
4. D. Moazed, *Mol. Cell.* **8**, 489 (2001).
5. R. A. Frye, *Biochem. Biophys. Res. Commun.* **273**, 793 (2000).
6. J. Min, J. Landry, R. Sternblitz, R.-M. Xu, *Cell* **105**, 269 (2001).
7. Q. She *et al.*, *Proc. Natl. Acad. Sci. U.S.A.* **98**, 7835 (2001).
8. Supplementary material is available on *Science Online* at www.sciencemag.org/cgi/content/full/296/5565/148/DC1.
9. J. C. Tanny, D. Moazed, *Proc. Natl. Acad. Sci. U.S.A.* **98**, 415 (2001).
10. J. C. Tanny, G. J. Dowd, J. Huang, H. Hilz, D. Moazed, *Cell* **99**, 735 (1999).
11. P. Forterre, F. Confalonieri, S. Knapp, *Mol. Microbiol.* **32**, 669 (1999).
12. S. D. Bell, S. S. Cairns, R. L. Robson, S. P. Jackson, *Mol. Cell* **4**, 971 (1999).
13. C. P. Magill, S. P. Jackson, S. D. Bell, *J. Biol. Chem.* **276**, 46693 (2001).
14. This work was funded by the Medical Research Council, BBSRC and Cancer Research Campaign. M.F.W. is a Royal Society University Research Fellow. We thank L. Ko Ferrigno for help preparing this manuscript.

4 February 2002; accepted 27 February 2002

Crystal Structure of the Extracellular Segment of Integrin $\alpha V\beta 3$ in Complex with an Arg-Gly-Asp Ligand

Jian-Ping Xiong,¹ Thilo Stehle,^{1,2*} Rongguang Zhang,^{3*}
Andrzej Joachimiak,³ Matthias Frech,⁴ Simon L. Goodman,⁵
M. Amin Arnaout^{1†}

The structural basis for the divalent cation-dependent binding of heterodimeric $\alpha\beta$ integrins to their ligands, which contain the prototypical Arg-Gly-Asp sequence, is unknown. Interaction with ligands triggers tertiary and quaternary structural rearrangements in integrins that are needed for cell signaling. Here we report the crystal structure of the extracellular segment of integrin $\alpha V\beta 3$ in complex with a cyclic peptide presenting the Arg-Gly-Asp sequence. The ligand binds at the major interface between the αV and $\beta 3$ subunits and makes extensive contacts with both. Both tertiary and quaternary changes are observed in the presence of ligand. The tertiary rearrangements take place in βA , the ligand-binding domain of $\beta 3$; in the complex, βA acquires two cations, one of which contacts the ligand Asp directly and the other stabilizes the ligand-binding surface. Ligand binding induces small changes in the orientation of αV relative to $\beta 3$.

Integrins are adhesion receptors that mediate vital bidirectional signals during morphogenesis, tissue remodeling, and repair [reviewed in (1)]. These heterodimers are formed by the noncovalent association of an α and a β subunit, both type I membrane proteins with large extracellular segments. In mammals, 18 α and 8 β subunits assemble into 24 different receptors. Integrins depend on divalent cations to bind their extracellular ligands. Although these ligands are structurally diverse, they all use an acidic residue during integrin recognition. Specificity for a particular ligand is then determined by additional contacts with the integrin. High affinity binding of

integrins to ligands is usually not constitutive but is elicited in response to cell "activation" signals (so-called "inside-out" signaling) that alter the tertiary and quaternary structure of the extracellular region, making the integrin ligand-competent. Ligand binding, in turn, induces structural rearrangements in integrins that trigger "outside-in" signaling [reviewed in (2)].

Integrins are grouped into two classes based on the presence or absence of an extracellular ~ 180 amino acid A-type domain (αA) (3). In the nine αA -containing integrins (αA -integrins), αA is necessary and sufficient for the divalent cation-dependent binding to physiologic ligands (3). The structures of isolated αA domains in "liganded" and "unliganded" conformations (4–8) have revealed how this domain interacts with ligands. A metal ion is coordinated at the ligand-binding interface of αA through a conserved five amino acid motif, the metal ion-dependent adhesion site (MIDAS), and the metal coordination is completed by a glutamate from the ligand (4, 6) or, in its absence, by a water molecule (9). In αA -lacking integrins, ligand recognition requires an αA -like

domain (βA) present in all integrin β subunits (4, 10).

The crystal structure of the extracellular segment of the αA -lacking integrin $\alpha V\beta 3$ was previously determined in the presence of Ca^{2+} ($\alpha V\beta 3$ -Ca) (10). It consists of 12 domains assembled into an ovoid head and two "legs." The putative ligand-binding head is primarily formed of a seven-bladed β -propeller domain from αV and a βA domain from $\beta 3$. These two domains resemble the $G\beta$ and $G\alpha$ subunits of G-proteins, respectively, and contact each other in a strikingly similar manner (10). We now report the structure of extracellular $\alpha V\beta 3$ in complex with the cyclic pentapeptide ligand Arg-Gly-Asp-{D-Phe}-{N-methyl-Val-}, called cyclo(RGD=N{Me}V [P5 in (11)], and in the presence of the proadhesive cation Mn^{2+} , $\alpha V\beta 3$ -RGD-Mn (Table 1). We have also determined the structure of the unliganded receptor in the presence of Mn^{2+} ($\alpha V\beta 3$ -Mn) for comparison (Table 1). The two structures contain the previously reported extracellular residues of the integrin (10). $\alpha V\beta 3$ -Mn contains six Mn^{2+} ions (replacing each of the six Ca^{2+} ions in $\alpha V\beta 3$ -Ca), and $\alpha V\beta 3$ -RGD-Mn contains the cyclic pentapeptide plus eight Mn^{2+} ions. Replacement of Ca^{2+} with Mn^{2+} at all six sites in the $\alpha V\beta 3$ -Mn structure did not result in important structural rearrangements in the integrin. As with $\alpha V\beta 3$ -Ca (10), no metal ion is visible at MIDAS in $\alpha V\beta 3$ -Mn. Figure 1 shows representative electron density maps (Fig. 1, A through D) and a ribbon diagram (Fig. 1E) of the integrin-pentapeptide complex.

The $\alpha V\beta 3$ -RGD-Mn structure reveals that the pentagonal peptide inserts into a crevice between the propeller and βA domains on the integrin head (Fig. 1E). The Arg-Gly-Asp, or RGD, sequence makes the main contact area with the integrin, and each residue participates extensively in the interaction, which buries 355 \AA^2 or 45% of the total surface area of the peptide. The Arg and Asp side chains point in opposite directions, exclusively contacting the propeller and βA domains, respectively. The five $C\alpha$ atoms of the cyclic peptide form a slightly distorted pentagon. Molecular dynamics simulations of the peptide in the absence of the integrin, performed using the same geomet-

¹Renal Unit, Leukocyte Biology and Inflammation Program, Structural Biology Program, Massachusetts General Hospital, 149 13th Street, Charlestown, MA 02129, USA. ²Laboratory of Developmental Immunology, Massachusetts General Hospital, and Harvard Medical School, 55 Fruit Street, Boston, MA 02114, USA. ³Argonne National Laboratory, Biosciences Division, Structural Biology Center, IL 60439, USA. ⁴Department of Target Research, ⁵Biomedical Research, Oncology, Merck KGaA, Darmstadt 64271, Germany.

*These two authors contributed equally to this work.
†To whom correspondence should be addressed. E-mail: arnaout@receptor.mgh.harvard.edu